CO_2 Sequestration in Bedded Sandstone-Shale Sequences

Tianfu Xu, John A. Apps, and Karsten Pruess

Earth Sciences Division, Lawrence Berkeley National Laboratory
University of California, Berkeley, CA 94720

Abstract. Alteration of the host rock aluminosilicate minerals is very slow under ambient deep-aquifers conditions and is not amenable to laboratory experiment. We therefore developed a numerical model of CO_2 injection in bedded sandstone-shale sequences using hydrogeologic properties and mineral compositions commonly encountered in Gulf Coast sediments. Simulations were performed with the reactive fluid flow and geochemical transport code TOUGHREACT, to analyze mass transfer between sandstone and shale layers, and CO_2 immobilization through carbonate precipitation. The geochemical evolution under both natural and CO_2 injection conditions was studied. The simulation results of mineral alteration under natural conditions agree well with field observations. Limited information currently available for the mineralogy of high-pressure CO_2 reservoirs is also generally consistent with our simulation. Results indicate that the pattern of mass transfer of aqueous chemical components under high CO_2 pressure conditions is different from that under natural conditions. Most CO_2 sequestration occurs in the sandstone. The major CO_2 trapping minerals are dawsonite and ankerite. The CO_2 mineral-trapping capacity after 100,000 years reaches 90 kg per cubic meter of medium. The addition of CO_2 mass as secondary carbonates to the sandstone results in decreased porosity. The leaching of chemical components from the shale increases porosity.

1. Introduction

A possible means of reducing carbon dioxide (CO_2) emissions to the atmosphere is injection of CO_2 into structural reservoirs in deep permeable geologic formations. Such formations could include aquifers, oil and gas fields, and coal seams. Aquifers are the most abundant fluid reservoirs in the subsurface. The deepest aquifers in the United States commonly contain brackish or saline water. Aquifers with salinities exceeding 10,000 mg/L total dissolved solids are excluded by the U.S. Environmental Protection Agency as underground sources of drinking water. Hence, they are logical targets for the eventual disposal of CO_2.

Numerical modeling of geochemical processes is necessary to investigate long-term CO_2 injection in deep aquifers, because aluminosilicate mineral alteration is very slow under ambient deep-aquifer conditions and is not amenable to experimental study. Xu et al. (2003a) present a geochemical modeling analysis of the interaction of aqueous solutions under high CO_2 partial pressures with three different rock types. The first rock is a glauconitic sandstone from the Alberta Sedimentary Basin. The second rock type evaluated is a proxy for a sediment from the United States Gulf Coast. The third rock type is a dunite, an essentially monomineralic rock consisting of olivine.

Xu et al. (2003b) performed reactive transport simulations of a 1-D radial well region under CO_2 injection conditions in order to analyze CO_2 immobilization through carbonate precipitation in Gulf Coast sandstones of the Frio formation of Texas. Most of the simulated mineral alteration pattern is consistent with the observations. Some inconsistencies with field observations are noted. For example, quartz abundance declines over the course of the simulation, whereas quartz overgrowths are observed during diagenesis due to the release of SiO_2 during replacement of smectite by illite in adjacent shales (Land, 1984).

Simplifications made in the previous modeling (Xu et al., 2003a and b) include: (1) treating the sandstone aquifer as if it were a closed system isolated from the enclosing shales, and (2) not adequately representing the extremely complex process of kerogen decomposition (or petroleum maturation) in deeply buried sediments. Here we present simulations on mass transfer, mineral alteration, and consequent CO_2 sequestration in a sandstone-shale system that overcome these simplifications. The mineral compositions of sandstone and shale are abstracted from Gulf Coast sediments. The mineralogy, thermodynamic database and kinetic data are refined from previous studies (Xu et al., 2003a and b).

2. Numerical Modeling Approach

2.1. Simulation method

The present simulations were carried out using the non-isothermal reactive geochemical transport code TOUGHREACT (Xu and Pruess, 2001). This code was developed by introducing reactive chemistry into the framework of the existing multi-phase fluid and heat flow code TOUGH2 (Pruess, et al., 1999). Our modeling of flow and transport in geologic media is based on space discretization by means of integral finite differences (Narasimhan and Witherspoon, 1976). An implicit time-weighting scheme is used for the individual components of the model consisting of flow, transport, and kinetic geochemical reactions. TOUGHREACT uses a sequential iteration approach similar to Yeh and Tripathi (1991). After solution of the flow equations, the fluid velocities and phase saturations are used for chemical transport simulation. The chemical transport is solved on a component basis. The resulting concentrations obtained from the transport are substituted into the chemical reaction model. The system of chemical reaction equations is solved on a grid-block basis by Newton-Raphson iteration, similar to Parkhurst et al. (1980), Reed (1982), and Wolery (1992). The chemical transport and reaction equations are iteratively solved until convergence. Full details on the numerical methods are given in Xu and Pruess (2001).

2.2. Processes

The simulator can be applied to one-, two-, or three-dimensional porous and fractured media with physical and chemical heterogeneity, and can accommodate any number of chemical species present in liquid, gas and solid phases. A wide range of subsurface thermo-physical-chemical processes is considered. The major processes considered for fluid and heat flow are: (1) fluid flow in both liquid and gas phases under pressure and gravity forces, (2) capillary pressure effects for the liquid phase, and (3) heat flow by conduction, convection and diffusion. Transport of aqueous and gaseous species by advection and molecular diffusion is considered in both liquid and gas phases. Aqueous chemical complexation and gas (CO_2) dissolution and exsolution are assumed to be locally at equilibrium. Mineral dissolution and precipitation can be modeled subject to either local equilibrium or kinetic conditions. Dissolution and precipitation of all minerals in simulations presented in this paper are assumed to be kinetically-controlled. The rate law used is from Steefel and Lasaga (1994). The activity of aqueous species is equal to the product of the activity coefficient and molar concentration (mol/kg H_2O). Aqueous species activity coefficients with the exception of CO_2(aq) are calculated from the extended Debye-Hückel equation (Helgeson et al., 1981). CO_2(aq) activity coefficient and CO_2(g) fugacity coefficient are functions of pressure, temperature and salinity (details on calculations are given in Xu et al. (2003a)).

Changes in porosity and permeability due to mineral dissolution and precipitation can modify fluid flow. This feedback between flow and chemistry can be important and can be considered in our model. Alternatively, the model can monitor changes in porosity and permeability during the simulation from changes in mineral volume fractions without feedback to the fluid flow. Changes in porosity during the simulation are calculated from changes in mineral volume fractions. Several models were considered to calculate changes in permeability due to changes in porosity. In the present work, the following are also neglected: (1) compaction and thermal mechanics; (2) the effect of chemical concentration changes on fluid thermophysical properties such as density and viscosity which are otherwise primarily dependent on pressure and temperature; (3) the enthalpy due to chemical reactions.

3. Problem Setup

3.1. Sandstone-shale configuration

A basic issue is the mass transfer and geochemical behavior in bedded sandstone-shale sequences under natural and high CO_2 pressure conditions. A simplified 1-D model of a sandstone-shale system is used (Figure 1). Hydrological parameter specifications for sandstone and shale layers were chosen to be representative of conditions that may be encountered in Texas Gulf Coast sediments at a depth of order 2 km. Details on parameters used are given in Xu et al. (2003c). The model grid becomes finer in the shale near the interface between sandstone and shale to better resolve concentration gradients in the low permeability shale. Only one grid block was used for the sandstone layer and the calculation point for this block was placed on the interface. This represents a conceptual model of perfect mixing throughout the sand, which can be justified on the basis of dispersion from regional groundwater flow.

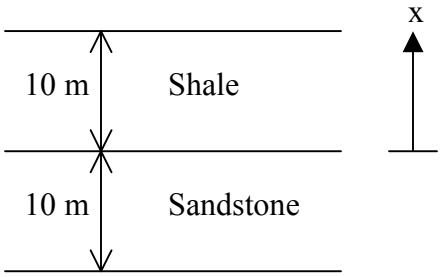

Figure 1. Simplified conceptual model for a sandstone-shale system.

3.2. Geochemistry

The specification of formation mineralogy is determined in part by the availability of data. Most studies related to the Tertiary Gulf Coast sediments are concentrated in the state of Texas. The principal reservoir-quality sandstones within that region are respectively, the Frio, the Vicksberg and the Wilcox formations, all of which are found within the Lower Tertiary. Of the three formations, the Frio was chosen as a representative candidate for the sequestration of supercritical carbon dioxide. The initial mineral composition of sandstone used in the present modeling (Table 1), was taken from the previous batch geochemical modeling study by Xu et al. (2003a). A detailed description of the sandstone mineralogy is given in Xu et al. (2003a).

The model shale composition is based on the recent study by Land et al., (1997) of Upper Oligocene - Lower Miocene mudrocks obtained at depths between 2130 and 5490 m from the Mobil #406 State Tract well in Kenedy County, Texas. The mineralogical analyses of Land et al. (1997) were plotted versus depth, and linearly regressed to obtain a functional relation with depth. Not all trends were linear, and slightly better fits were obtained in some cases with second order polynomial equations despite the substantial scatter in the data. However, only the linear correlations were used, and these were extrapolated incrementally to a depth of 2,000 m, corresponding to an approximate ambient temperature of approximately 75 °C. The mineralogical concentrations (Wt.%) were converted to specific volumes (m^3/mol) and normalized to 98 vol.%, the balance of 2 vol.% being assigned to organic matter, i.e. kerogen-OS. More details on the shale mineralogy are given in Xu et al. (2003c).

The thermodynamic properties of several phases such as carbonates, chlorite and kerogen-OS were refined during this study from previous modeling (Xu et al., 2003 a and b). Further details on thermodynamic and kinetic data used are given in Xu et al. (2003c).

Table 1. List of initial mineral volume fractions and possible secondary mineral phases for sandstone and shale layers.

Mineral	Chemical composition	Vol.%	
		Sandstone	Shale
***Primary*:**			
quartz	SiO_2	57.888	19.220
kaolinite	$Al_2Si_2O_5(OH)_4$	2.015	4.371
calcite	$CaCO_3$	1.929	10.901
illite	$K_{0.6}Mg_{0.25}Al_{1.8}(Al_{0.5}Si_{3.5}O_{10})(OH)_2$	0.954	28.140
kerogen-OS	$C_{64}H_{102}O_{40}S_{10}$	0.0	2.0
oligoclase	$CaNa_4Al_6Si_{14}O_{40}$	19.795	5.293
K-feldspar	$KAlSi_3O_8$	8.179	4.746
Na-smectite	$Na_{0.290}Mg_{0.26}Al_{1.77}Si_{3.97}O_{10}(OH)_2$	3.897	23.023
chlorite	$Mg_{2.5}\ Fe_{2.5}Al_2Si_3O_{10}(OH)_8$	4.556	2.3516
hematite	Fe_2O_3	0.497	0.0
***Secondary*:**			
low-albite	$NaAlSi_3O_8$		
dolomite	$CaMg(CO_3)_2$		
siderite	$FeCO_3$		
Ca-smectite	$Ca_{0.145}Mg_{0.26}Al_{1.77}Si_{3.97}O_{10}(OH)$		
pyrite	FeS_2		
ankerite	$CaMg_{0.3}Fe_{0.7}(CO_3)_2$		
dawsonite	$NaAlCO_3\ (OH)_2$		

Prior to the reactive transport simulations in the sandstone-shale system, batch geochemical modeling of water-rock interaction for individual sandstone and shale was performed to obtain a nearly equilibrated water chemistry, using a pure 1.0 M solution of sodium chloride and CO_2 gas pressure of 1×10^{-2} bar reacting with the primary minerals listed in Table 1 at a temperature of 75 ^oC. The resulting water chemistry was used for the initial condition of reactive geochemical transport simulations under natural as well as CO_2 injection scenarios.

Two reactive geochemical transport simulations were performed. The first simulation was for water-rock interaction under natural conditions without CO_2 injection at a temperature T = 75^oC. The system always remains in single-phase liquid conditions for the natural simulation. The second simulation considers a CO_2 pressure of 201 bars based on the assumption that the injection occurs about 2 km deep (T = 75^oC). The high CO_2 pressure (due to injection) is assumed to initially occur only in the sandstone. The CO_2 gas pressure is assumed to be in equilibrium with the solution at all times. The geochemical transport simulations were run for a period of 100,000 years.

4. Results and Discussion

4.1. Natural conditions

Some of the results obtained under natural conditions are presented in Figures 2 and 3. More results can be found in Xu et al. (2003c). For sandstone, the initial pH (Figure 2a) is 7.34, for shale it is slightly lower (6.69) due to kerogen-OS decomposition. H^+ diffuses from shale to sandstone, with eventual establishment of uniform pH. Ca^{+2} (Figure 2b), and total carbonate (Figure 2d) also diffuse from the shale to sandstone. Kerogen-OS dissolves steadily and constantly in the shale, which buffers the pH. Oligoclase and K-feldspar are destroyed very rapidly in both shale and sandstone layers. Calcite (Figure 3a) dissolves in the shale and a dissolution peak is formed about 2 m from the interface, and precipitates in the sandstone. Na-smectite (Figure 3b) dissolution occurs in the sandstone and in the shale close to the interface. Chlorite dissolves throughout both domains especially inside the shale. Quartz (Figure 3c) precipitates in the sandstone but remains essentially at equilibrium within the shale. Illite (Figure 3d) precipitates due to dissolution of oligoclase and K-feldspar. Pyrite precipitates steadily due to the release of sulfide by dissolving kerogen-OS.

The results of mineral alteration for the natural state agree well with field obvervations. The formation of quartz overgrowths in the sandstone is observed during diagenesis due to the release of SiO_2 during replacement of smectite by illite in adjacent shales (Land, 1984). This phenomenon is reproduced

by the current modeling. Dissolution of organic matter, oligoclase, K-feldspar, Na-smectite and chlorite, pyrite, calcite, low-albite, and illite are also well reproduced by the simulation. Further details on comparison can be found in Xu et al. (2003c). The interaction between sandstone and shale layers improves significantly the results compared with the previous work where the diagenesis of sandstone was isolated from the enclosing shales (especially for quartz, pyrite and chlorite).

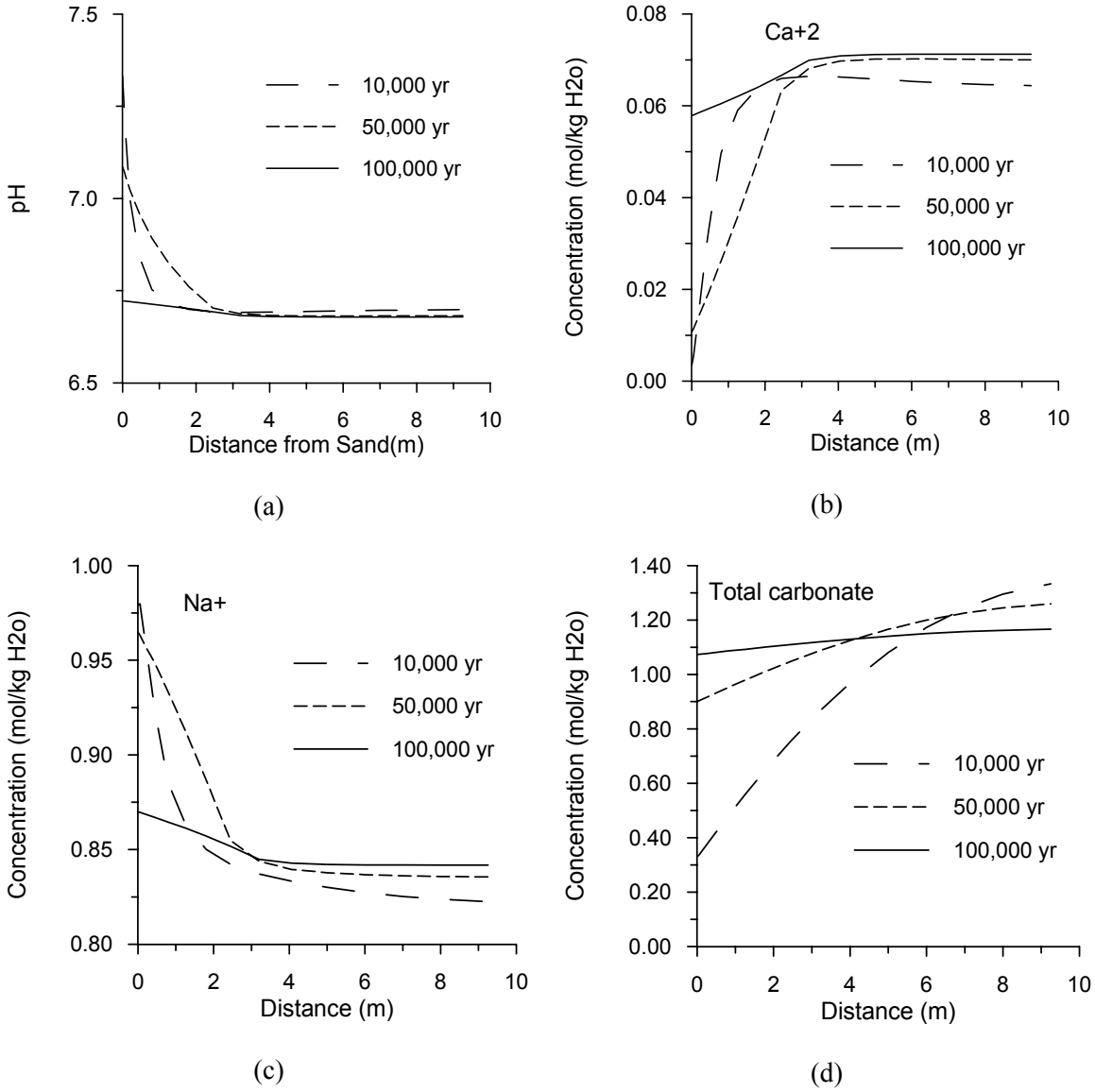

Figure 2. Concentrations of aqueous chemical component under natural conditions. Note that scales are different among figures.

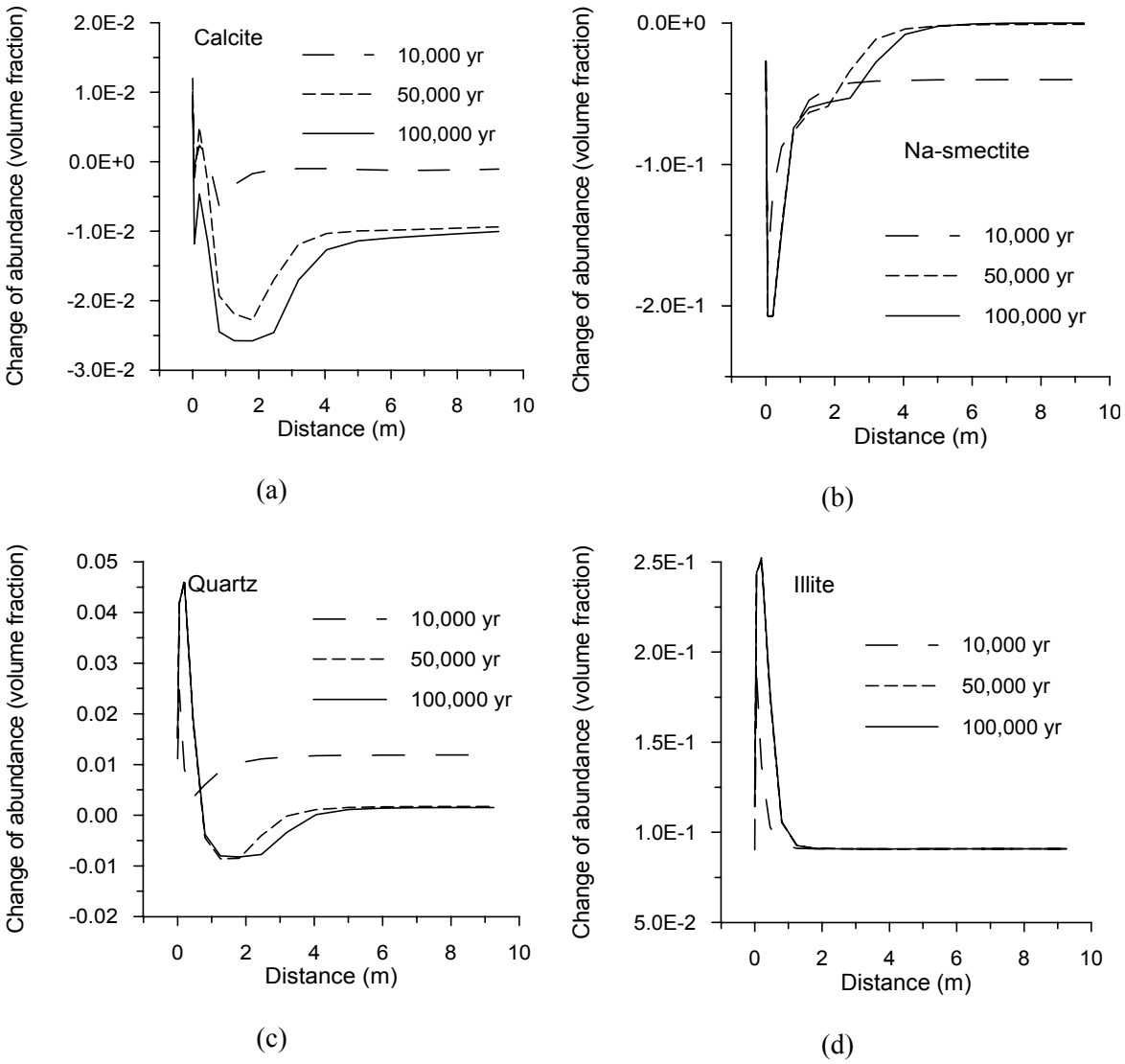

Figure 3. Change of mineral abundance (negative values indicate dissolution and positive precipitation) under natural conditions.

4.2. High CO_2 pressure conditions

The results obtained under high CO_2 pressure conditions are presented in Figures 4 through 6. With the imposition of a high CO_2 pressure of 201 bars, a lower pH of 5.3 (Figure 4a) is reached in the sandstone. H^+ diffuses from the sandstone to shale, which is opposite to natural conditions. Ca^{+2} (Figure 4b) initially diffuses from the shale into the sandstone, but later reverses direction and diffuses from the sandstone to shale. Na^+ (Figure 4c) in contrast to Ca^{+2}, initially diffuses from the sandstone to shale, but later reverses direction. Total iron (Figure 4d) behaves similarly to Ca^{+2} due to significant precipitation of ankerite (Figure 5c) in the sandstone. The behavior of other chemical components also differs from that under natural conditions.

Dissolution of kerogen-OS and precipitation of pyrite in the shale are the same as those of the first simulation. The change of calcite abundance (Figure 5a) is different, dissolving slightly in the sandstone instead of precipitating as under natural conditions. This is because a lower pH is obtained under high CO_2 pressure conditions. Chlorite (Figure 5b) dissolution under high CO_2 conditions is much larger in both layers, and is driven by ankerite precipitation. Siderite precipitates initially, but later dissolves, and finally disappears, because of competition for Fe with ankerite. Ankerite (Figure 5c) and dawsonite (Figure 5d) precipitation occurs mostly in the sandstone and in the shale close to the interface due to the presence of high pressure CO_2. The latter two carbonate minerals are not observed in the

natural condition simulation. An increase of porosity is observed in the interior of the shale and a decrease in the sandstone and in the region close to the interface, indicating mass leaching from the shale.

Most CO_2 sequestration occurs in the sandstone. Evolution of carbonate mineral abundances in the sandstone is presented in Figure 6a. The major CO_2 trapping minerals are dawsonite and ankerite. Siderite precipitates initially, but later dissolves in favor of ankerite, until disappearance. Calcite precipitates initially but later dissolves continuously. Dolomite is not formed in the current simulation. Cumulative CO_2 sequestration in the sandstone (Figure 6b) increases gradually until about 40,000 years, and then slows. The trend is consistent with that of carbonate mineral precipitation and dissolution. The CO_2 mineral-trapping capacity after 100,000 years reaches 90 kg per cubic meter medium.

Field observations concerning the mineralogy and geochemistry of natural high-pressure CO_2 reservoirs are sparse, and therefore even qualitative model validation is difficult. However, the limited information currently available is generally consistent with our simulation.

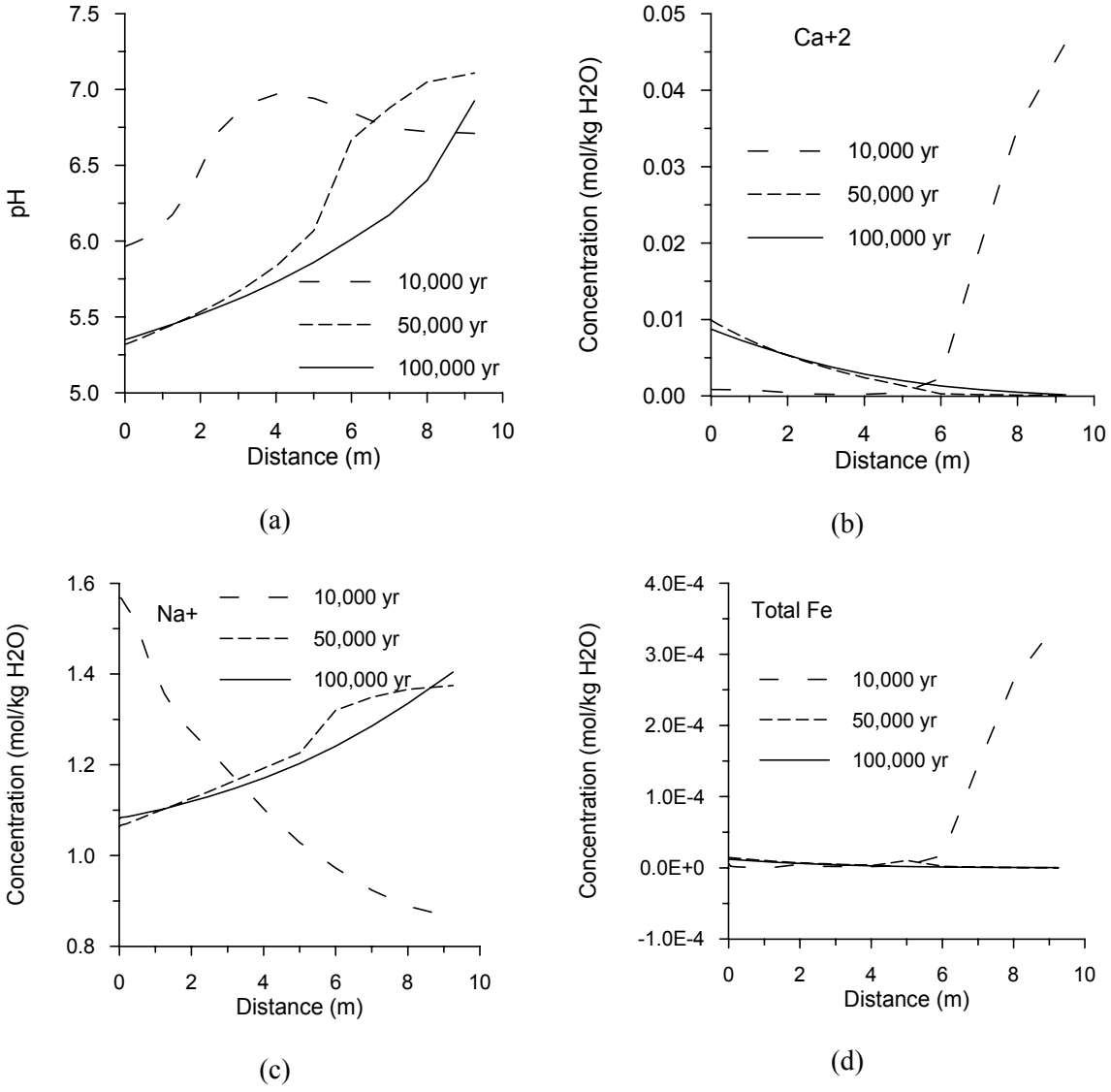

Figure 4. Concentrations of aqueous chemical components under high CO_2 pressure conditions.

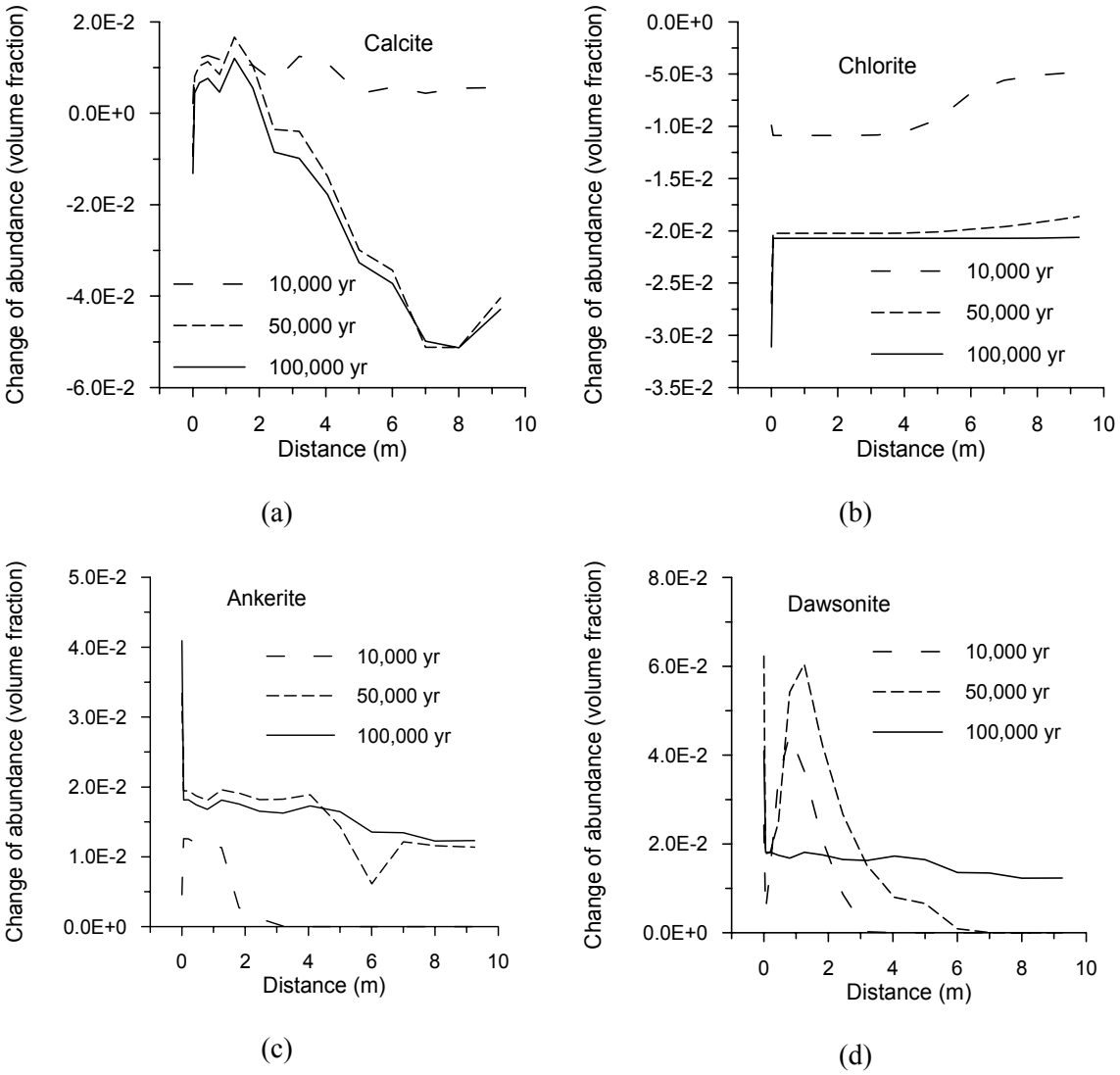

Figure 5. Change of mineral abundance (negative values indicate dissolution and positive precipitation) under high CO_2 pressure conditions.

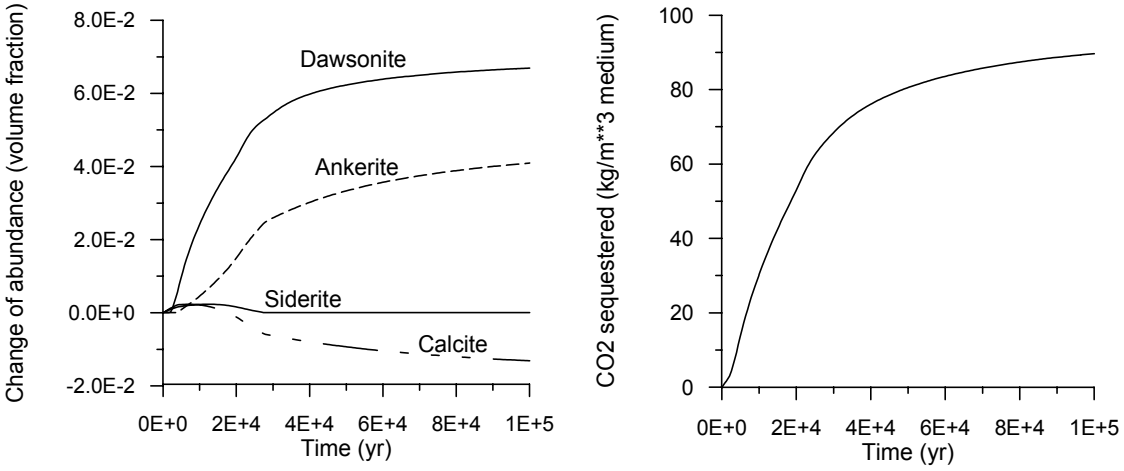

(a) Change of carbonate abundance

(b) Cumulative CO_2 sequestration

Figure 6. Time evolution in the sandstone under high CO_2 pressure conditions.

5. Summary and Conclusions

A reactive geochemical transport model for a sandstone-shale system has been developed to simulate both natural and high CO_2 pressure conditions. The model has been used to analyze mass transfer of aqueous chemical components, the alteration pattern of minerals, and sequestration of CO_2 by secondary carbonates for a Gulf Coast aquifer.

The simulation under natural conditions is validated by field observations of the diagenesis of Gulf Coast sediments, and in particular, sandstones of the Frio formation of Texas. The simulation results of mineral alteration agree well with field obvervations. Dissolution of organic matter, oligoclase, K-feldspar, Na-smectite and chlorite, and precipitation of quartz, pyrite, calcite, low-albite, and illite are well reproduced by the simulation. Considering the interaction between sandstone and shale layers improves significantly the results compared with the previous work where the diagenesis of sandstone was isolated from the enclosing shales (especially for quartz, pyrite and chlorite). Limited information currently available for the mineralogy of natural high-pressure CO_2 reservoirs is also generally consistent with our simulation.

The pattern of mass transfer of aqueous chemical components under CO_2 injection conditions differs from that under natural conditions. H^+ diffuses from the sandstone to shale, which is opposite to the natural conditions. Ca^{+2} initially diffuses from the sandstone to shale but later reverses direction. Na^+ in contrast to Ca^{+2}, initially diffuses from the shale to sandstone, but later reverses direction. Total iron behaves similarly to Ca^{+2}, due to significant precipitation of ankerite in the sandstone.

Most CO_2 sequestration occurs in the sandstone. The major CO_2 trapping minerals are dawsonite and ankerite. The CO_2 mineral-trapping capacity after 100,000 years reaches 90 kg per cubic meter medium. The addition of CO_2 mass as secondary carbonates to the sandstone results in decreased porosity. Leaching chemical mass from the shale causes increased porosity.

The model investigated here assumes perfect mixing throughout the sand layer, due to larger groundwater velocities there. Future work should examine the interplay between sand and shale interaction locally and regional groundwater flow in more detail, including the possibility of groundwater flow in the sandstone being sufficiently slow so that chemical gradients may develop in the sandstone as a function of distance from the interface with the shale.

Acknowledgement. We thank Curtis Oldenburg and Keni Zhang for reviews of the manuscript. This work was supported by the Director, Office of Science, Office of Basic Energy Sciences, of the U.S. Department of Energy, under Contract No. DE-AC03-76SF00098 with Lawrence Berkeley National Laboratory.

References

Helgeson, H.C., Kirkham, D.H., Flowers, G.C., 1981. Theoretical prediction of the thermodynamic behavior of aqueous electrolytes at high pressures and temperatures: IV. Calculation of activity coefficients, osmotic coefficients, and apparent molal and standard and relative partial molal properties to 600 C and 5 kb. Am. J. Sci. 281, 1249–1516.

Land, L.S., 1984. Frio sandstone diagenesis, Texas Gulf Coast: A regional isotopic study. In Clastic Diagenesis, (David A. McDonald and Ronald C. Surdam, Eds.) AAG Memoir 37, Part 1. Concepts and Principles, 47-62.

Land, L.S., Mack, L.E., Milliken, K.L., Lynch, F.L., 1997. Burial diagenesis of argillaceous sediment, south Texas Gulf of Mexico sedimentary basin: A reexamination. GSA Bulletin 109(1), 2-15.

Narasimhan, T.N., Witherspoon, P.A., 1976. An integrated finite difference method for analyzing fluid flow in porous media, Water Resour. Res. 12, 57–64.

Parkhurst, D.L., Thorstenson, D.C., Plummer, L.N., 1980. PHREEQE: A computer program for geochemical calculations: US Geological Survey, Water Resources Investigation 80-96, 174 pp.

Pruess, K., Oldenburg, C., Moridis, G., 1999. TOUGH2 user's guide, Version 2.0. Lawrence Berkeley Laboratory Report LBL-43134, Berkeley, California.

Reed, M.H., 1982. Calculation of multicomponent chemical equilibria and reaction processes in systems involving minerals, gases and aqueous phase. Geochim. et Cosmochim. Acta 46, 513-528.

Steefel, C.I., Lasaga, A.C., 1994. A coupled model for transport of multiple chemical species and kinetic precipitation/dissolution reactions with applications to reactive flow in single phase hydrothermal system. Am. J. Sci. 294, 529-592.

Wolery, T.J., 1992. EQ3/6: Software package for geochemical modeling of aqueous systems: Package overview and installation guide (version 7.0). Lawrence Livermore National Laboratory Report UCRL-MA-110662 PT I, Livermore, California.

Xu, T., Pruess, K., 2001, Modeling multiphase non-isothermal fluid flow and reactive geochemical transport in variably saturated fractured rocks: 1. Methodology, Am. J. Sci., 301, 16-33.

Xu, T, Apps, J.A., Pruess, K., 2003a. Numerical simulation to study mineral trapping for CO_2 disposal in deep aquifers, Applied Geochemistry, in press.

Xu, T, Apps, J.A., Pruess, K., 2003b. Reactive geochemical transport simulation to study mineral trapping for CO_2 disposal in deep arenaceous formations, Journal of Geophysical Research 108(B2).

Xu, T, Apps, J.A., Pruess, K., 2003c. Mass transfer, mineral alteration and CO_2 sequestration in a sandstone-shale system, Lawrence Berkeley National Laboratory Report LBNL-52566, Berkeley, California, 46 pp.

Yeh, G.T., Tripathi, V.S., 1991. A model for simulating transport of reactive multispecies components: model development and demonstration. Water Resour. Res. 27, 3075-3094.